DESIGN AND ANALYSIS OF ISLANDING DETECTION WITH REACTIVE POWER DISTURBANCE FOR INVERTER-BASED DISTRIBUTED GENERATORS

[1]RAJARAPU.SRAVANTHI, [2]SINGAM SRIDHAR
[1]M.tech, BALAJI INSTITUTE OF TECHNOLOGY&SCIENCE
[2]Assistant Professor, BALAJI INSTITUTE OF TECHNOLOGY&SCIENCE

Abstract-The main objective of the paper is islanding detection method for inverter which is based upon the distributed generators (DGs) is explained in the paper, which is also based upon the perturbing reactive power output. In this method two sets of disturbances are configured, along with the different duration time and amplitudes. Therefore the first set of reactive power disturbance (FSORPD) is periodic along with the small amplitudes which are to break the reactive power balance during islanding, whereas the magnitude of the second set of reactive power disturbance (SSORPD) is sufficient to force the frequency to deviate outside its threshold limits. After islanding, the possible frequency variation characteristics along with the FSORPD may have three criterions which are designed for switching the disturbance from the FSORPD to the SSORPD. Therefore DG is located at various positions which may have the same frequency variation characteristics, the SSORPDs can be added on various DGs at the same time without the need of communication. Moreover the synchronization of the SSORPDs may be guaranteed for the system along with the multiple DGs and the method can detect islanding with a zero no detection zone property. Simulation results verify that the proposed method performs well on islanding detection.

Index Terms—Disturbance synchronization, inverter-based distributed generation, islanding detection, reactive power disturbance

I. INTRODUCTION

This paper is deal about the Islanding which have the condition in which a portion of the utility system can consist of both the DG and load along with the continues operating during this portion is electrically which is separated from the main utility. Islanding can be result in power quality problems, serious equipment damage, and even safety hazards to utility operation personnel and many more. Therefore the maximum delay may be 2 s which is required for the detection of an islanding and a generic system for islanding detection study is recommended as well, where the distributed network, the RLC load and the DG are connected at the point of common coupling (PCC).

Islanding detection methods are divided into following three categories: 1) active methods; 2) communication-based methods; and3) passive methods. Therefore the communication based methods may not have the harmful effect to the power quality of the power system and it may not have the non detection zones (NDZs) in the theory. However, the cost is much increase because of the need of communication infrastructure and the operations are more complex as well.

Therefore to decrease or eliminate the NDZ, active methods rely on intentionally injecting disturbances, negative sequence components or harmonics into some DG parameters to identify whether islanding has occurred. Though active methods suffer smaller NDZs, they sacrifice power quality and reliability of the power system during normal operation. Moreover, some active methods have difficulty in maintaining synchronization of the intentional disturbances. Therefore, they may not work owing to the averaging effect when applied in multiple-DG operation.

The main aim of this paper is too inspired for the studies. So the main objective is an islanding detection method which is depends upon the intermittent bilateral reactive power variation (RPV) which has been proposed. Therefore the variation in the amplitude is about 5% of the DG's active power output. The frequency was eventually forced to deviate outside the normal range during islanding due to the reactive power variation. When Compared with the method and the method proposed and it was improved by only outputting unilateral RPV in each variation period and further reducing the variation amplitude based on the load's resonance frequency detection.

The proposed method has following three distinguishing features: 1) It can be applied to the DG either operating at unity power factor or supplying reactive power as well for its local load; 2) Synchronization of the disturbances can be guaranteed for the system with multiple DGs and the method can detect islanding with the zero NDZ property; 3) The perturbation of reactive power is further reduced during normal operation.

II. BASIC RELATIONSHIP ANALYSIS AND RPV METHODS

A. System Modeling and Basic Relationship Analysis

According to the recommended test system for islanding detection study is shown in Fig. 1. As shown in Fig. 1(a), when the DG is connected to the utility grid, the following equations describe the

power flows and the active and reactive power consumed by the load:

$$P_{Load} = P_{DG} + P_{Grid} = 3\frac{V_{PCC}^2}{R} \quad (1)$$

$$Q_{Load} = Q_{DG} + Q_{Grid} = 3V_{PCC}^2\left(\frac{1}{2\pi fL} - 2\pi fC\right) \quad (2)$$

Where VPCC and f are the phase voltage at the PCC and its frequency, and R, L, C represents the load resistance, inductance, and capacitance, respectively.

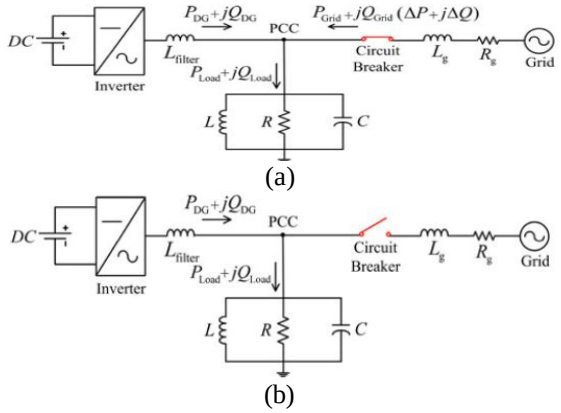

Fig. 1. Test system for islanding detection study (a) Grid-connected operation mode (b) Islanding operation mode

It consists of an inverter-based DG, a parallel RLC load and the grid represented by a source behind impedance. The operation mode of the DG depends on whether the circuit breaker is closed or not

Fig. 2 presents the block diagram of the DG interface control. The phase-locked loop (PLL), the outer power control loop and the inner current control loop are three main parts

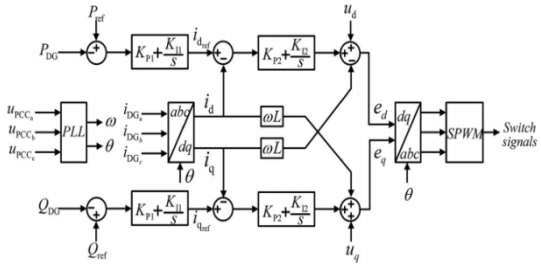

Fig. 2. DG interface control for constant power operation.

Moreover, the load's resonant Frequency (*f*0) and quality factor (*If*) can be expressed as

$$Q_f = R\sqrt{\frac{C}{L}} = 2\pi f_o RC \quad (3)$$

$$f_o = \frac{1}{2\pi\sqrt{LC}} \quad (4)$$

According to IEEE Std.929, *Qf* is typically set at 2.5. By combining (1), (3), and (4), (2) can be rewritten as follows:

$$Q_{Load} = P_{Load}Q_f\left(\frac{f_o}{f} - \frac{f}{f_o}\right) \quad (5)$$

On the other hand, when islanding occurs as shown in Fig. 1(b), it can be inferred from (1) that if the active power mismatch ΔP(ΔP = PLoad − PDG = PGrid) is not equal to zero, the PCC voltage will fall or rise no matter the DG operates at unity power factor or not. The amount of voltage deviation depends on the value of ΔP. If the active power reference of the DG is set to be constant, ΔP can be expressed as follows.

$$\Delta P = P_{DG}\left(\frac{1}{(1+\Delta V)^2} - 1\right) \quad (6)$$

Where ΔV represents the voltage deviation and it can be expressed as

$$\Delta V = \frac{V_{PCC.i} - V_{PCC}}{V_{PCC}} \quad (7)$$

Where VPCC and VPCC.i represent the PCC voltage before and after islanding, respectively. If the active power mismatch is not large enough, the passive OVP/UVP method will suffer the NDZ due to inadequate changes of the PCC voltage. Thus, the frequency variation also can be used to detect islanding based on the OFP/UFP method.

According to (5), the load's reactive power consumption after islanding (QLoad.i) can be expressed as follows:

$$Q_{Load.i} = Q_{DG} = P_{Load.i}Q_f\left(\frac{f_o}{f_i} - \frac{f_i}{f_o}\right)$$

$$= P_{DG}Q_f\left(\frac{f_o}{f_i} - \frac{f_i}{f_o}\right) \quad (8)$$

Where PLoad.i and fi represent the load's active power consumption and the frequency of the PCC voltage after islanding, respectively. The DG operating at unity power factor does not generate reactive power. According to (8), the needed reactive power disturbance to force the frequency to deviate from fi to its target value (Qdis) can be expressed as follows:

$$Q_{dis} = P_{DG}Q_f\left(\frac{f_o}{f_i + \Delta f} - \frac{f_{i+\Delta f}}{f_o}\right) \quad (9)$$

Where Δf represents the frequency deviation and it can be expressed as

$$\Delta f = f_{i.tar} - f_i \quad (10)$$

Where fi.tar represents the target frequency and it can be set at any value that is out of the frequency's normal range. For the DG operating at unity power factor, assuming that PDG is equal to 1, Fig. 3 illustrates the relationship between fi and Qdis with fi.tar being set at the threshold values.

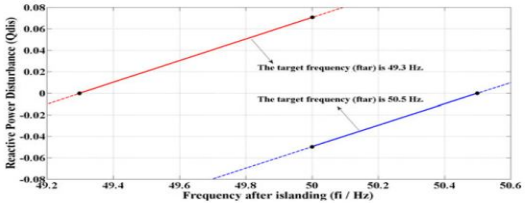

Fig. 3. Relationship between *fi* and *Q*dis for the DG operating at unity power factor.

However, the relationship between Qdis and Δf should be modified when the DG supplies both active and reactive power for the local load. If there are no power mismatches, the frequency will not change after islanding. According to (8), Qdis for the DG of this kind can be expressed as follows

$$Q_{dis} = P_{DG}Q_f\left(\frac{f_o}{f_{i.tar}} - \frac{f_{i.tar}}{f_o}\right) - P_{DG}Q_f\left(\frac{f_o}{f_i} - \frac{f_i}{f_o}\right)$$
$$= -P_{DG}Q_f\Delta f\left(\frac{f_o}{f_i(f_i+\Delta f)} + \frac{1}{f_o}\right) \quad (11)$$

Condition 1: Assuming that PDG is equal to 1 and f0 is equal to 50 Hz, Fig. 4 illustrates the relationship between fi and Qdis with fi.tar being set at the threshold values.

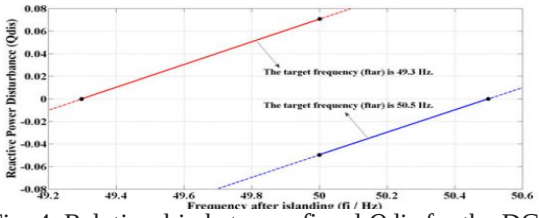

Fig. 4. Relationship between *fi* and *Q*dis for the DG generating both active and reactive power (*f*0 is set at 50 Hz).

Compared with Fig. 3, Fig. 4 shows approximately the same Qdis–fi curve. Condition 2: Assuming that PDG is equal to 1 and fi is equal to 50 Hz, Fig. 5 illustrates the relationship between f0 and Qdis with fi.tar being set at the threshold values. It can be seen from Fig. 5.

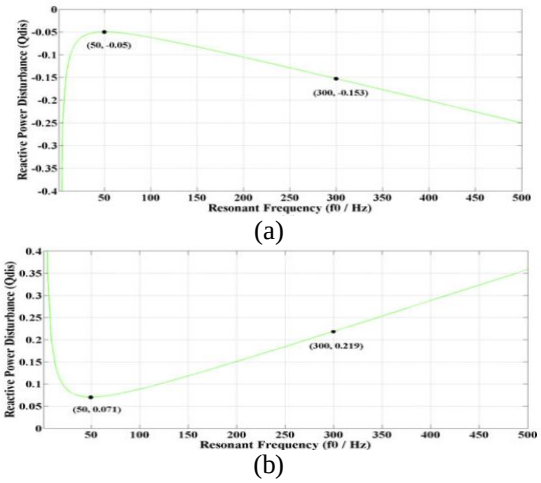

Fig. 5. Relationship between *f*0 and *Q*dis for the DG generating both active and reactive power (a) *fi* and *fi*tar are set at 50 Hz and 50.5 Hz, respectively (b) *fi* and *fi*tar are set at 50 Hz and 49.3 Hz, respectively.

Therefore, following two important conclusions can be obtained: 1) for the load whose resonant frequency f0 is actually unknown in advance, the calculated Qdis might be not sufficient enough to drive fi to deviate to fi.tar with f0 being set at 50 Hz in (11) and 2) for the same load, the frequency variation with f0 being set at 300 Hz is about three times as much as that with f0 being set at 50 Hz.

B. Islanding Detection Methods Proposed

Based on the RPV Owing to the smaller disturbance amplitude analyzed previously, islanding detection methods based on the reactive power disturbance might be better choices than those based on the active power disturbance.

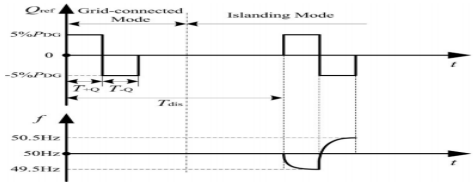

Fig. 6. *Q*ref and corresponding frequency in both operation modes with the method proposed

Fig. 6 illustrated Qref and corresponding frequency in both grid-connected and islanding modes, respectively.

According to, Qref for the DG in different frequency conditions was shown in Fig. 7. For the DG operating at unity power factor, the rated value of Qref is zero.

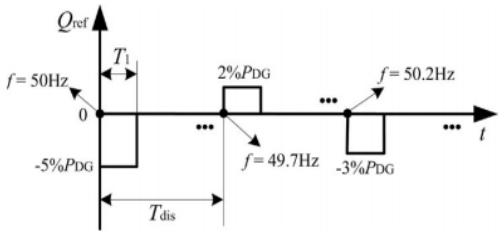

Fig. 7. Reactive power reference of the DG with different values of the frequency.

However, when they were applied to multiple DGs, the synchronization of the variations could not be guaranteed in both methods. Owing to the averaging effect, they might fail to detect islanding for the system with multiple DGs.

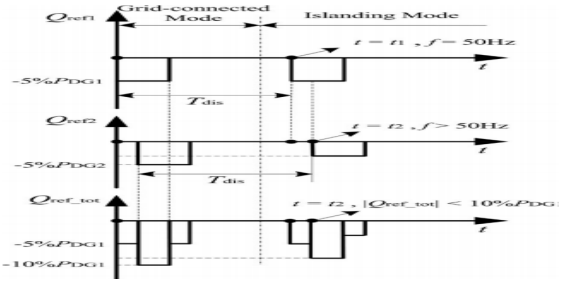

Fig. 8. Separate and total reactive power variations for the system with twoDGs according to the method

According to the method in Fig. 8 illustrated the separate and total reactive power variations for the system with two DGs, where the reactive power variation on the DG2 lagged behind that on the DG1 and f0 is 50 Hz. Therefore, when islanding occurred, the variation on the DG1 forced the frequency to

increase earlier and the frequency was larger than 50 Hz when the variation on the DG2 started. Accordingly, the magnitude of the variation on the DG2 was less than 5%PDG2.

III. PROPOSED ISLANDING DETECTION METHOD BASED ON REACTIVE POWER DISTURBANCE

In order to improve the performance of islanding detection methods that are based on the reactive power disturbance, following three problems have to be solved: 1) the method has to be applicable for both the DG operating at unity power factor and that generating reactive power as well; 2) the disturbance on the DG is better to be reduced as much as possible during normal operation and it also has to be sufficient to drive the frequency outside its threshold limits after islanding; and 3) the synchronization of the disturbances on different DGs has to be guaranteed.

In addition, the design of the FSORPD also has to comply with following two principles: 1) reducing disturbance as much as possible during normal operation and 2) forming criterions for starting the SSORPD after islanding. In order to meet aforementioned requirements, the FSORPD is designed to contain two parts whose amplitudes are Qdis1 and 2Qdis1, respectively, and it is added on the DG's rated reactive power reference periodically. The value of Qdis1 is equal to either Qdis11 or Qdis12, which depends on the frequency at the beginning of the FSORPD. Fig. 9 illustrates the FSORPD with different values of f and corresponding frequency variation during islanding, respectively. The FSORPD causes the sudden mismatch of the reactive power during islanding and accordingly there is a transient response of the frequency.

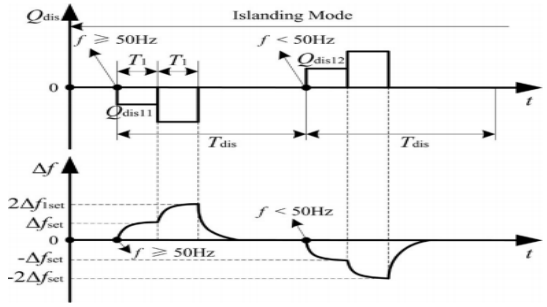

Fig. 9. FSORPD with different values of *f* and corresponding frequency variation during islanding.

There are two possible conditions that the FSORPDs are asynchronous: 1) the overlap region exists among the FSORPDs on several DGs and 2) the FSORPD on a certain DG does not overlap with the FSORPDs on the other DGs.

Moreover, the value of Twin has to be either equal to that of T1 or no more than that of (T1 − Ttra). Therefore, (16) is configured as the third criterion for disturbance switching. The aforementioned three criterions for switching the disturbance from the FSORPD to the SSORPD are shown in Table I.

TABLE I
CRITERIONS FORSWITCHING THEDISTURBANCEFROM THEFSORPDTO THESSORPD

criterion	content	Corresponding condition
First	1)f >50.3Hz or f<49.7Hz;2)its duration time is no less than T_{dur}	The FSORPDs are synchronous or the non synchronization is not serious
Second	1)the SOAFV is periodic ;2) its cycle time is equal to T_{dis}	1)The FSORPDs are asynchronous 2)some FSORPDs overlap with each other
Third	1)the SOAFV satisifies equation ;2) the frequency variation is not zero	1)The FSORPDs are asynchronous 2)a certain FSORPDs overlap with each other

TABLE II CRITERIONS FOR ISLANDING DETERMINATION

criterion	content	Suitable application
First	1)f >50.5Hz or f<49.3 Hz;2) its duration time is no less than T_{dur} .	1)the DG operating qt unity power factor ;2) the DG generating both active and reactive power
Second	1)the SOAFV satisfies equation ;2) the frequency variation is not zero	The DG generating both active and reactive power

The second and third criterions complement each other, which can reduce the starting time of the SSORPD. Moreover, these two criterions reflect the frequency variation characteristics corresponding to the FSORPD during islanding.

In case of no islanding switching evens, which may transiently impose a significant frequency deviation as well, the duration time of above abnormal frequency condition has to be no less than Tdur to determine islanding. It has to be noted that the SSORPD is not periodic. If the SSORPD is activated by false islanding, it will be replaced by the FSORPD again after its duration. As for the DG generating both active and reactive power simultaneously, f0 is unknown in advance and it cannot be calculated after islanding.

TableIII
Time Variables and Their Meanings

Time Variable	Meaning
T_1	The duration time of each part in both the FSORPD and the SSORPD.
T_{dis}	The period time of the FSORPD.
T_{win}	The measurement window size for SOAFV calculation.
T_{tra}	The transient time of frequency deviation from a steady value to another steady one.
T_{dur}	The duration time of the abnormal frequency state.

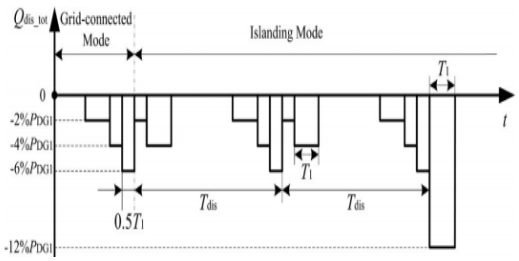

Fig. 10. Schematic diagram of the maximum islanding detection time.

Assuming that the active power references of two DGs are same (PDG1 = PDG2) and the FSORPD on the DG2 lags 1.5T1 behind that on the DG1, Fig. 10 illustrates the maximum detection time of the proposed method when islanding occurs. The FSORPD on the DG2 overlaps with that on the DG1. As shown in Fig. 10, when islanding occurs, the total reactive power disturbance (Qdisto t) just misses its maximum value.

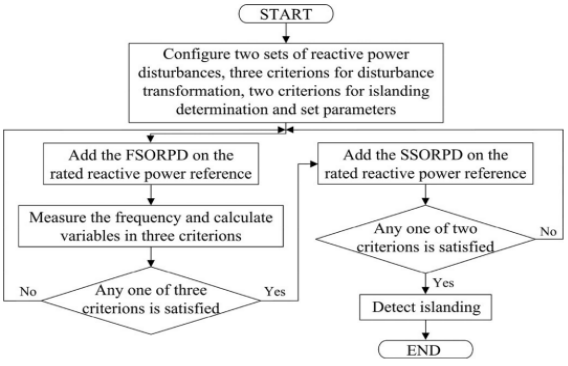

Fig. 11. Flowchart of the proposed islanding detection method

Generally, the FSORPD is added on the rated reactive power reference of the DG. If any of three criterions for disturbance switching is satisfied, the SSORPD will take the place of the FSORPD.

Constant RLC load is generally considered as the hardest detectable condition for an islanding detection method and it is recommended in the generic system to examine the islanding detection methods' performance.

IV. PERFORMANCE OF THE PROPOSED ISLANDING DETECTION METHOD

In this section, several test cases are simulated on the power systems computer-aided design (PSCAD)/Electro magnetic transient in DC system (EMTDC) based on the system in Fig. 1.

A. Performance of the Proposed Method for the DG Operating at Unity Power Factor

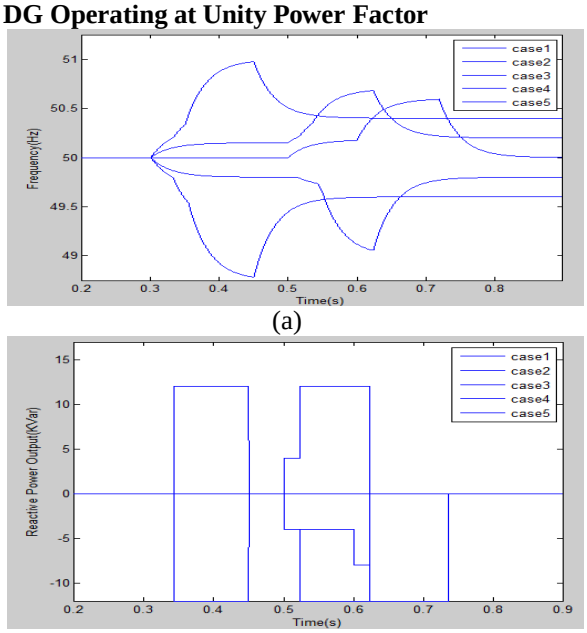

(a)

Fig. 12. Simulation results for loads with different values of *f*0 during islanding (a) The PCC frequency (b) The DG's reactive power output.

It can be noted from Fig. 12(a) that frequencies deviate outside the threshold limits in all five cases and islanding can be detected with different detection time.

Table IV
Simulation Results for Different Test Cases Part A

Case	f_0/Hz	Startup time of the SSORPD/ms	Detection result	Detection time/ms
1	50	324	detected	356
2	50.2	226	detected	245
3	50.4	42	detected	60
4	49.8	224	detected	260
5	49.6	42	detected	70

Based on case 1 in Table V, following three conditions are considered: 1) in case A, only the resistance of phase a is set at 97% of its rated value; 2) in case B, only the resistance of phase c is set at 103% of its rated value; 3) in case C, resistances of phase a and phase c are set at 97% and 103% of the rated value, respectively. With the DG adopting the general constant power control strategy, the PCC frequency and the DG's reactive power output during islanding in each aforementioned test case are shown.

Table V
Parameters of the Study System

	Parameters	Values
Grid	Voltage	400 V
	Frequency	50 Hz
	Grid Resistance	0.1 Ω
	Grid Inductance	1.5915 mH
DG Inverter Controller	K_{p1}/K_{i1}	0.025/2
	K_{p2}/K_{i2}	1.5/0.01
	P_{ref}	200 kW

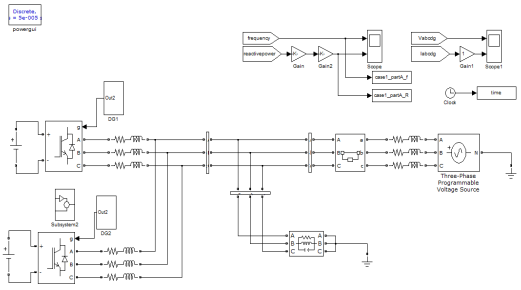

Fig.13 Block diagram of simulation

Table VI
Load Parameter Setting For Different Test Cases in Part A

Case	R/Ω	L/mH	C/μF	f_0/Hz
1	0.8	1.0186	9947.2	50
2	0.8	1.0145	9907.6	50.2
3	0.8	1.0105	9868.2	50.4
4	0.8	1.0227	9987.1	49.8
5	0.8	1.0268	10027.4	49.6

It can be inferred from Fig. 13(a) that frequencies in all three cases eventually deviate outside the upper threshold 50.5 Hz and the duration time of this condition is longer than 10 ms. Moreover, it also can be seen from Fig. 13(a) that the fluctuation range of the PCC frequency is larger for the more unbalanced load.

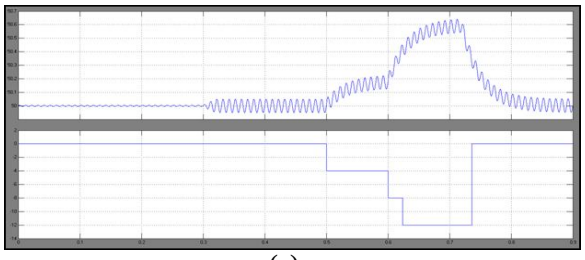

(a)

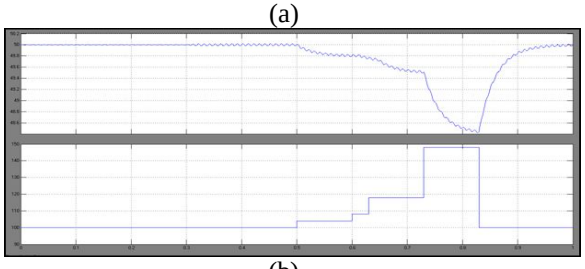

(b)

Fig. 14. Simulation results for unbalanced loads (a) The PCC frequency (b) The DG's reactive power output

B. Performance of the Proposed Method for the DG Generating Active and Reactive Power Simultaneously

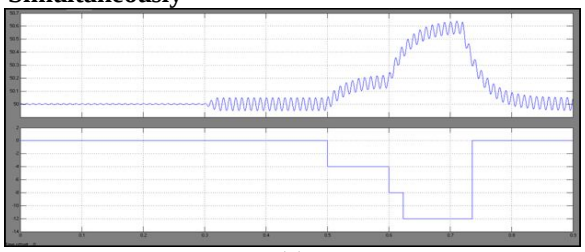

(a)

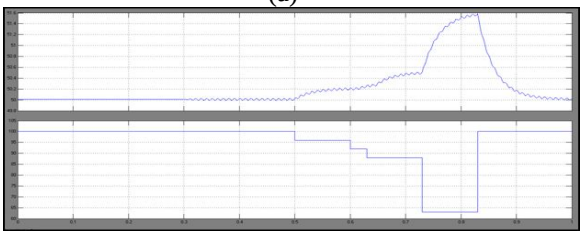

(b)

Fig. 15. Simulation results during islanding for the DG generating active and reactive power simultaneously (a) The PCC frequency (b) The DG's reactive power output.

Table VII
Load Parameter Setting For Different Test Cases In Part B

Case	R/Ω	L/mH	C/μF	f_0/Hz	ΔP_{nor}/kW	ΔQ_{nor}/kVar
1	0.8	0.9218	9002.1	55.3	0	0
2	0.7619	0.9218	9002.1	55.3	10	0
3	0.8421	0.9218	9002.1	55.3	−10	0
4	0.8	0.9145	8930.7	55.7	0	8
5	0.8	0.9292	9074.1	54.8	0	−8

ΔPnor and ΔQnor in Table VII represent the active power mismatch and the reactive power mismatch between the DG and the load during normal operation, respectively. Fig. 15 illustrates the PCC frequency and the DG's reactive power output during islanding in each case of Part B. Accordingly, compared with the frequency in case 1, it can be seen from Fig. 15(a) that the frequency starts to descend in case 2 or rise in case 3 once islanding occurs. As shown in Fig. 15(a), frequencies in these five cases have been in the steady state at t = 0.96 s.

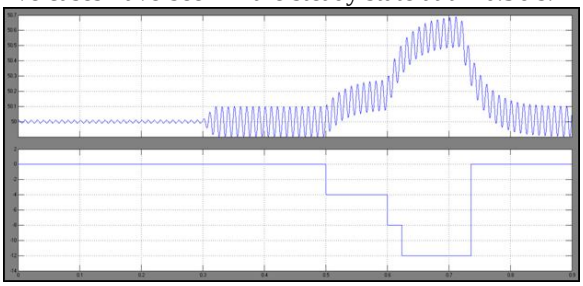

(a)

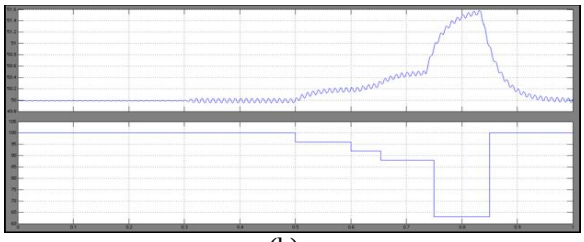

(b)

Fig. 16. Simulation results for unbalanced loads (a) The PCC frequency (b) The DG's reactive power output.

Fig. 16 shows the simulation results in these three cases. It can be seen from Fig. 16(a) that frequencies in all three conditions deviate outside the threshold limits and the duration time of this condition is longer than 10 ms.

C.Comparison of the Performance of the Proposed Method with that of the Methods for the DG Operating at Unity Power Factor under Multiple-DG Operation Mode

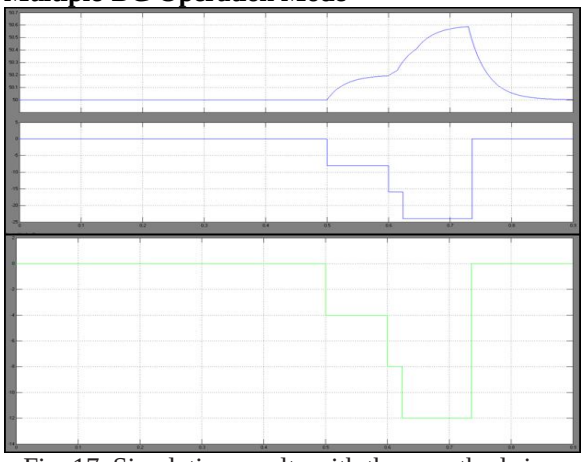

Fig. 17. Simulation results with three methods in scenario A (a) The PCC frequency (b) Separate reactive power output (c) The DG's total reactive power output.

For comparison, this situation is simulated as well in scenario B. Fig. 17 shows the PCC frequency and the DGs' total reactive power output in scenario A according to different methods. It can be seen from Fig. 16(a) that islanding can be detected with all these three methods in this scenario. Fig. 18 illustrates the simulation results in scenario B with the lag time equal to 80 ms.

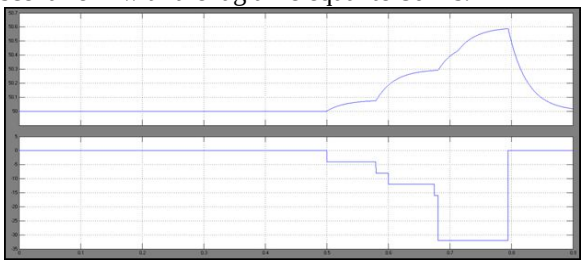

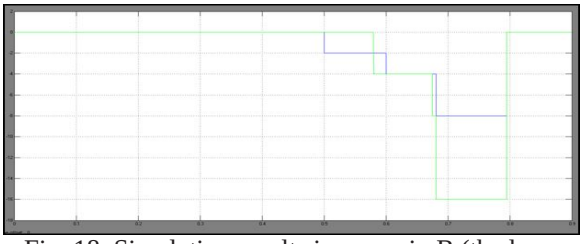

Fig. 18. Simulation results in scenario B (the lag time is 80 ms) (a) The PCC frequency (b) Separate reactive power output (c) The DG's total reactive power output.

However, it can be seen from Fig. 18 that the overlap part of the FSORPDs can still drive the frequency to be larger than 50.3 Hz with the method proposed in this paper, thus the SSORPDs are added on both DGs synchronously.

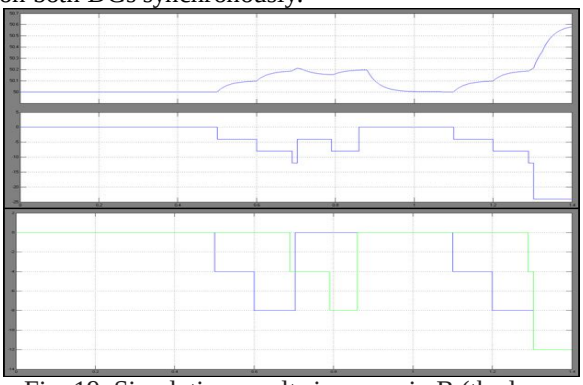

Fig. 19. Simulation results in scenario B (the lag time is 180 ms) (a) The PCC frequency (b) Separate reactive power output (c) The DG's total reactive power output

Fig. 19 illustrates the PCC frequency and the DGs' total reactive power output in scenario B with the lag time equal to 180 ms. as shown in Fig. 18, the maximum value of the frequency caused by this overlap part is 50.26 Hz, which is less than 50.3 Hz.

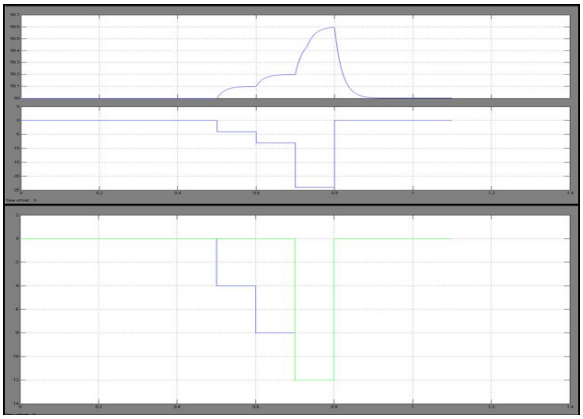

Fig. 20. Simulation results with three methods in scenario C (a) The PCC frequency (b) Separate reactive power output (c) The DG's total reactive power output.

CONCLUSION

In this paper, during the constant power control, the inverter based DG can generate the both reactive and active power simultaneously; therefore this paper may observe the relation among the reactive power disturbance and the frequency variation during islanding. The proposed method may consist of two sets of reactive power disturbances. They also have the various duration time and magnitude for various purposes. Moreover the magnitudes of the FSORPD are less so which may decrease the impact on the system during normal operation. Therefore, DGs may be located at various positions which can detect the similar frequency variation characteristics no matter what the operation mode is, which guarantees the synchronization of the SSORPDs on different DGs without the need of communication. Therefore accordingly to the proposed method it can be reliably and effectively detect islanding for the multiple-DG operation. This paper is verifying simulation result of the proposed method by using the mat lab/simulink.

REFERENCES

[1] H. B. Puttgen, P. R. MacGregor, and F. C. Lambert, "Distributed generation: Semantic hype or the dawn of a new era?," IEEE Power Energy Mag., vol. 1, no. 1, pp. 22–29, Jan./Feb. 2003.

[2] P. P. Barker and R. W. de Mello, "Determining the impact of distributed generation on power systems: Part 1—Radial distribution systems," in Proc. IEEE Power Eng. Soc. Summer Meeting, Jul. 2000, pp. 1645–1656.

[3] IEEE Recommended Practice for Utility Interface of Photovoltaic (PV) Systems, IEEE Standard 929-2000, Apr. 2000.

[4] IEEE Standard for Interconnecting Distributed Resources with Electric Power Systems, IEEE Standard 1547-2003, Jul. 2003.

[5] R. A. Walling and N. W. Miller, "Distributed generation islanding— Implications on power system dynamic performance," in Proc. IEEE Power Eng. Soc. Summer Meeting, Jul. 2002, pp. 92–96.

[6] G. Hernandez-Gonzalez and R. Iravani, "Current injection for active islanding detection of electronically-interfaced distributed resources," IEEE Trans. Power Del., vol. 21, no.3, pp. 1698–1705, Jul. 2006.

[7] A. Timbus, A. Oudalov, and N. M. Ho Carl, "Islanding detection in smart grids," in Proc. IEEE Energy Convers. Congr. Expo., Sep. 2010, pp. 3631– 3637.

[8] D. Reigosa, F. Briz, C. Blanco, P. Garcia, and J. M. Guerrero, "Active islanding detection for multiple parallel-connected inverter-based distributed generators using high-frequency signal injection," IEEE Trans. Power Electron., vol. 29, no. 3, pp. 1192–1199, Mar. 2014.

[9] F. De Mango, M. Liserre, A. D. Aquila, and A. Pigazo, "Overview of antiislanding algorithms for PV systems. Part I: Passive methods," in Proc. IEEE Power Electron. Motion Control Conf., Aug. 2006, pp. 1878–1883.